JOURNAL OF MATERIALS SCIENCE **39** (2004) 3457–3460

# Synthesis and electrorheological effect of PAn–$BaTiO_3$ nanocomposite

J. H. WEI, J. SHI
*Department of Physics, Wuhan University, Wuhan 430072, People's Republic of China; International Center for Material Physics, CAS, Shenyang 110016, People's Republic of China*
*E-mail: jshi@whu.edu.cn*

J. G. GUAN, R. Z. YUAN
*State Key Laboratory of Advanced Technology for Materials Synthesis and Processing, Wuhan University of Technology, Wuhan 430070, People's Republic of China*

Electrorheological (ER) fluid is known as a smart liquid whose apparent viscosity can experience a rapid, reversible change upon application of an electric field. The ability to electrically control the apparent viscosity makes ER fluid potentially useful for numerous electromechanical devices such as valves, dampers, or clutches for the automotive or robotics industries [1–3]. Compared to a similar intelligent fluid, magnetorheological (MR) fluid, although ER fluid responds to the field more rapidly, its rather lower shear yield strength prevents it from widespread applications.

In order to obtain a material with improved electrorheological performance, we synthesized a new type of organic–inorganic nanocomposite made of polyaniline and barium titanate (PAn-$BaTiO_3$) by means of a modified organic–inorganic *in-situ* complex technique. Polyaniline was selected due to its advantages such as thermal stability at high temperature, low density, controllable conductivity, etc. [4, 5]. In addition, among sol–gel-derived materials, barium titanate ($BaTiO_3$), in particular, has large electronic resistance and excellent dielectric strength which makes it suitable to be used as ER material [6]. However, the high density, poor dispersion stability, and low shear stress confined its application. Recently, nanocomposites have gained great research interest as ER materials, such as polyamide-12/layered silicate nanocomposite [7]. PAn-Clay nanocomposite [8], polysaccharide/$TiO_2$ [9] nanocomposite, etc. The organic–inorganic nanocomposite not only can combine different kinds of material properties but also can reveal novel properties not existing in the constituent phases.

In this paper, the microstructure of PAn–$BaTiO_3$ nanocomposite particles was characterized by Fourier transform infrared (FT-IR) spectrum and X-ray photoelectron spectrum (XPS); the ER performance based on pure PAn, $BaTiO_3$ particles and PAn–$BaTiO_3$ nanocomposite particles with the various ratios of PAn and $BaTiO_3$ was investigated in detail.

The barium titanate superfine powder was made by routine sol–gel processing. In a typical preparation procedure of PAn-$BaTiO_3$ composite, 11.88 ml aniline was dissolved in 150 ml distilled water containing 25 ml hydrochloric acid. The solution was precooled at 0 °C, and the desired quantity of $BaTiO_3$ (ranging from 0 to 7.5 g) was added to the solution and stirred thoroughly. The ammonium peroxydissulfate (27.38 g, dissolved in 1.8 mol $l^{-1}$ HCl solution) was slowly added to the reaction mixture. During the synthesis, the mixtures were stirred at about 400–500 rmp for 8 hr and the temperature was kept at 0 °C. Afterward, the PAn-$BaTiO_3$ nanoparticles were obtained by dedoping (doping), washing, filtering, drying, milling, and sieving. The composites with different $BaTiO_3$ mass percents are shown in Table I. The $BaTiO_3$ mass percent came from thermal gravimetric-differential thermal analysis (TG-DTA) [10].

The FT-IR spectra of the mixture of PAn, $BaTiO_3$, and PAn-$BaTiO_3$ nanocomposites were recorded on a Nicolet 60 SXB spectrophotometer; the surface chemistry of PAn-$BaTiO_3$ nanocomposite was examined by XPS. The XPS measurements were carried out by the use of an ESCLAB MKII manufactured by VG Scientific Co. Nanocomposite particle density was determined by pycnometer using silicone oil as dispersing medium, and the density of the particles was measured to be 1.65–2.55 g/$cm^3$. The dielectric constants and conductivity of the particles were measured using an Agilent 4294A precision impedance analyzer.

The prepared particles were dried at 100 °C for 24 hr to remove any trace water, and then mixed quickly with dried silicone oil. The ER suspensions with 20 vol% of particles were prepared by magnetic stirring for 8 hr. Shear stress ($\tau$) versus external electric field was determined with HAAKE CV-20 Rheometer. All the experiments reported in this paper were performed at 30 °C.

Fig. 1 shows the FT-IR spectra of the nanocomposite and the mixture of PAn and $BaTiO_3$. It is interesting to notice that although the two spectra have approximate similarity, some differences can be observed in the spectra (see $*$ in Fig. 1). Comparing the FT-IR spectra of nanocomposite (Fig. 1a) with that of the mixture of PAn and $BaTiO_3$ (Fig. 1b), the peak in the spectrum of the mixture at 983 $cm^{-1}$ which is from the N—O stretching vibration shifts to 1101 $cm^{-1}$ in that of the composite; furthermore, two weak adsorption peaks in the spectrum of the mixture of PAn and $BaTiO_3$ near to 1147 $cm^{-1}$ from aromatic amine disappear in the spectrum of nanocomposite, instead of three obvious adsorption peaks near to 1147 $cm^{-1}$. We suppose these differences indicate the existence of a chemical bond between PAn and $BaTiO_3$ in the nanocomposite. In the

0022–2461 © *2004 Kluwer Academic Publishers* 

TABLE I Constitutes of PAn-$BaTiO_3$ nanocomposite

| PAn-$BaTiO_3$ nanocomposite | $BaTiO_3$ in composite (%) |
|---|---|
| PAn | 0 |
| PB-1 | 21.23 |
| PB-2 | 36.21 |
| PB-3 | 48.21 |
| PB-4 | 54.52 |

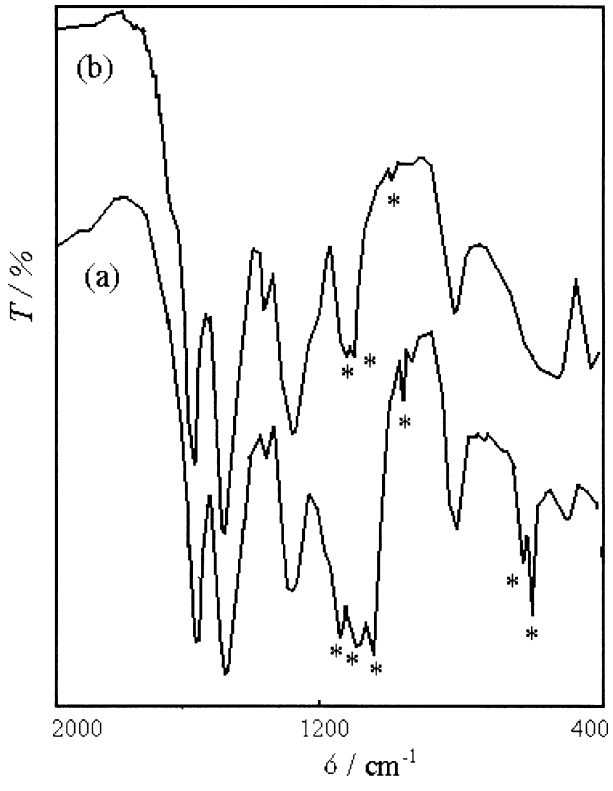


*Figure 1* FTIR spectra of: (a) PAn-$BaTiO_3$ nanocomposite and (b) the mixture of PAn and $BaTiO_3$.

host chain of the polymer, the effective doping point is −N= group when −NH− group and −N= group coexist. So, we can deduce that there are hydrogen bonds forming between PAn and $BaTiO_3$ in the composite which makes PAn and $BaTiO_3$ not easy to dissociate.

Besides the differences of the peaks location in the spectra of Fig. 1, the shape and strength also have some differences. The peaks near to 1147 $cm^{-1}$ from aromatic amine in the spectrum of the nanocomposite are broader than the corresponding ones in the mixture, and the intensity of the peaks in the spectrum of the nanocomposite is also strengthened compared with that of the mixture. These differences in the IR spectra can be explained on the basis of the constrained growth model of PAn grown in the presence of $BaTiO_3$ [11]. In such a case, the aniline monomer gets initially absorbed on the $BaTiO_3$ particles, that is, the polymerization process took place on the surface of these oxide particles when $(NH_4)_2S_2O_8$ is added to the solution, which leads to adhesion of the polyaniline to the $BaTiO_3$ particles and the constrained growth around these particles. It is just this kind of adsorption and constrained motion of the polymer chains that leads to the difference in the IR spectra. This deduction is consistent with the measurement result of XPS; the XPS result for the PAn-

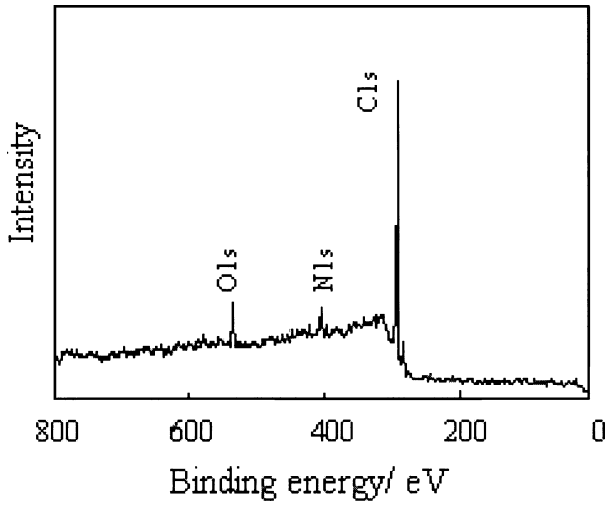


*Figure 2* XPS spectra of PAn-$BaTiO_3$ nanocomposite.

$BaTiO_3$ nanocomposite particles is shown in Fig. 2. Except the absorption peaks of $O_{1s}$ and $C_{1s}$ in the spectrum, $N_{1s}$ which is the representative absorption peaks of PAn can be seen clearly, but the absorption peak of $Ti_{2p}$ (459.9 eV) which is the representative absorption peaks of $BaTiO_3$ can hardly be found in the spectrum. Given that XPS is highly surface-specific technique with a typical analysis depth of 5–100 nm, these spectra should be representative of only the surfaces of the nanocomposite particles which are in intimate contact with the overlayer. Thus, it appears that the polyaniline synthesized with $BaTiO_3$ in the reaction mixture forms mainly on the oxide particle surface.

Fig. 3 shows the dependence of external electric field strength on shear stress of the ER fluids based on pure polyaniline, barium titanate, and the PAn-$BaTiO_3$ nanocomposite particles at $T = 30\,^{\circ}C$ and $\phi =$ 20 vol%. In the case of barium titanate, the shear stress is proportional to the field and a maximum of shear stress is 460 Pa obtained at $E = 3.5$ kV/mm. On the other hand, the suspensions of polyaniline particles are Newtonian and show a better ER effect than that of $BaTiO_3$ particles; its maximum shear stress is about 980 Pa at $E = 3.5$ kV/mm, which is perhaps due to the

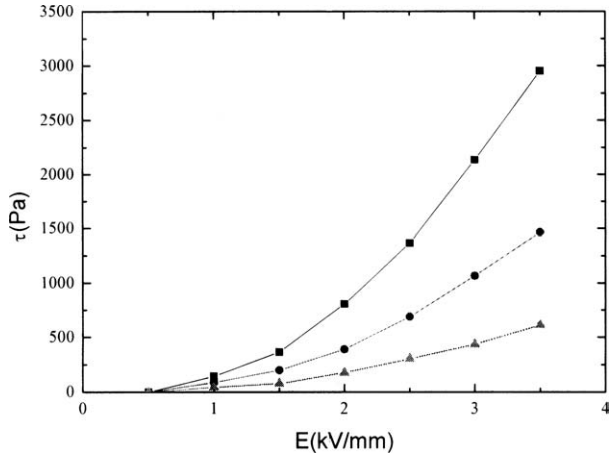


*Figure 3* The relationship between electric field and shear stress for ERF of different particles (■) PAn-$BaTiO_3$ nanocomposite, (●) PAn, (▲) $BaTiO_3$.

existence of the eonjugate $\pi$ bond in its structure so that the particles can be strongly polarized in the exterior electric field. Overall, the ER fluids based on PAn-$BaTiO_3$ nanocomposite particles show the strongest ER effect; its shear stress is about 2800 Pa at 3.5 kV/mm DC field, which is 6 times and 3 times larger than those of pure $BaTiO_3$ and PAn, respectively. According to the widely accepted issues of Davis and other researchers [12–14], large dielectric constant and suitable dielectric loss and conductivity ($\sim 10^{-7}$S/m) dominate the ER effect. The weak ER effect of the fluids with only $BaTiO_3$ particles has been attributed to its low conductivity according to the conduction model of ER mechanism [15, 16]. When $BaTiO_3$ particles compounded with PAn whose conductivity can be adjusted by demanding [17, 18], ER activity of the composite can be adjusted by controlling the electrical properties of the polymeric particles [10]. At the same experimental condition, because of the interaction of PAn and $BaTiO_3$, the composite particles show a stronger polarization strength and more polarization charges in the surface of the particles when an external electric field is applied. So, the ER effect of the nanocomposite is improved greatly.

Fig. 4a shows the shear stress of the ER fluids based on PAn-$BaTiO_3$ particles at $E = 3.0$ kV/mm as a function of conductivity with various mass percents of $BaTiO_3$. The ER effect obviously depends on the mass percent of $BaTiO_3$ and the particle conductivity; the highest yield stress is found at $BaTiO_3\% = 48.21\%$ and $\sigma = 10^{-7}\ \mathrm{S \cdot cm^{-1}}$. Fig. 4b shows the relationship between the conductivity ($\sigma_p$) and the dielectric constants ($\varepsilon_p$) of PAn-$BaTiO_3$ nanocomposite with various $BaTiO_3$ percentages. The $\varepsilon_p$ are calculated from formula

$$\varepsilon_p = \varepsilon_m(2 + V)/2(1 - V),$$

where $\varepsilon_m$ is the test dielectric constant value and $V$ is the porosity of the testing sample. The porosity is calculated according to the mass, density of nanocomposite particles, and the volume of used electrode box in the measurement process [19]. We find that the maximum dielectric constant can be obtained at $BaTiO_3\% = 48.21\%$ under a fixed conductivity. When $BaTiO_3\% > 50\%$ in the composite, the dielectric constant decreases with increasing $BaTiO_3\%$. Depending on the point-dipole approximation model [20, 21], the shear stress

$$\tau \propto kE^2\beta^2, \quad \beta = (\varepsilon_p - \varepsilon_c)/(\varepsilon_p + 2\varepsilon_c).$$

Here $k$ is a constant, $E$ is the applied electric field, $\varepsilon_p$ and $\varepsilon_c$ are the dielectric constants of dispersion particles and dispersion medium, respectively. The shear stress would increase linearly with the dielectric constant ratio ($\varepsilon_p/\varepsilon_c$), indicating that a high particle dielectric constant ($\varepsilon_p$) would give a strong ER effect. Our experimental result (Fig. 4a) is consistent with this model.

In summary, the PAn-$BaTiO_3$ nanocomposites were synthesized by inorganic–organic *in-situ* complex technique and their ER performance was investigated in detail. The FT-IR and XPS results show that the surfaces of the nanocomposite particles are mainly covered by polyaniline; there are hydrogen bonds forming between PAn and $BaTiO_3$ in the composite, which makes PAn and $BaTiO_3$ not easy to dissociate; the ER performance based on PAn-$BaTiO_3$ nanocomposite is much higher than that of pure polyaniline and barium titanate; the maximum yield stress can be obtained at $BaTiO_3\% = 48.21\%$ in the composite and $\sigma = 10^{-7}\ \mathrm{S \cdot cm^{-1}}$.

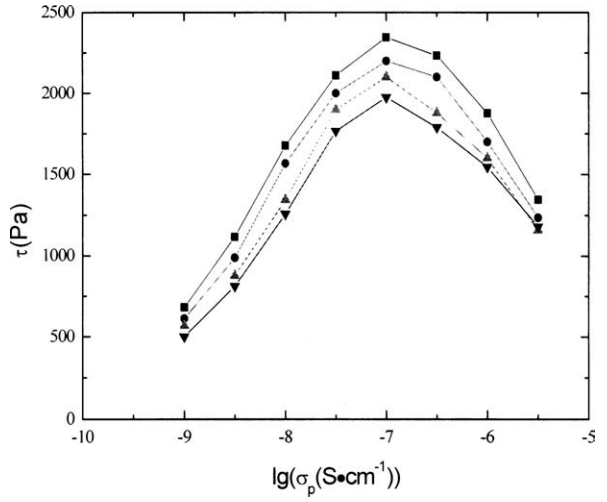


(a)

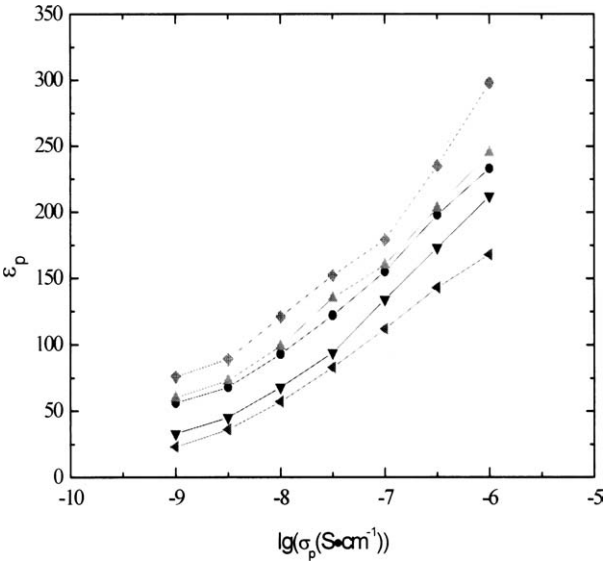


(b)

*Figure 4* (a) The relationship between conductivity and shear stress of PAn-$BaTiO_3$ nanocomposite with different $BaTiO_3$ percentage (■) PB-3, (●) PB-4, (▲) PB-2, (▼) PB-1. (b) The relationship between conductivity and dielectric constants of PAn-$BaTiO_3$ nanocomposite with different $BaTiO_3$ percentage (♦) PB-3, (▲) PB-4, (●)PB-2, (▼)PB-1, (◤) PAn.


## Acknowledgment

This work was supported by National Science Foundation of China (no. 59832090 & 10174056).


## References


1. R. TAO (ed.), Electrorheological Fluids, Magnetorheological Suspensions and Their Applications, in Proceedings of the 7th International Conference (Singapore, World Scientific) 2000.

2. M. NAKANO and K. KAYAMA (eds.), Electrorheological Fluids, Magnetorheological Suspensions and Their Applications, in Proceedings of the 6th International Conference (World Scientific, Singapore 1999).
3. T. C. HALSEY, *Science* **258** (1992) 273.
4. B. D. CHIN and O. O. PARK, *J. Colloid Interf. Sci.* **234** (2001) 344.
5. C. J. GOW and C. F. ZUKOSI, *ibid.* **136** (1990) 175.
6. A. KAREIVE, S. TAUTKUS and R. RAPALAVICIUTE, *J. Mater. Sci.* **34** (1999) 4853.
7. B. HOFFMANN, J. KRESSLER and G. STOPPELMANN, *Colloid Polym. Sci.* **278** (2000) 629.
8. Y. T. LIM, J. H. PARK and O. O. PARK, *J. Colloid Interf. Sci.* **245** (2002) 198.
9. X. P. ZHAO and X. DUAN, *ibid.* **251** (2002) 376.
10. J. H. WEI, Ph.D. Dissertation, Wuhan University of Technology, Wuhan 2002 (in Chinese).
11. P. R. SOMANI, R. MARIMUTHU, U. P. MULIK, S. R. SAINKAR and D. P. AMALNERKAR, *Synthetic Metals* **106** (1999) 45.
12. L. C. DAVIS, *J. Appl. Phys.* **72** (1993) 1334.
13. H. R. MA, W. J. WEN, W. Y. TAM and P. SHENG, *Adv. Phys.* **52** (2003) 343.
14. T. HAO, *Appl. Phys. Lett.* **70** (1997) 1956.
15. R. A. ANDERSON, Electrorheological Fluids, Mechanism, Properties, Structure, Technology, and Applications, in Proc. of the Int. Conf. on Electrorheological Fluids, Carbonale, Illinois, USA, World Scientific, Singapore, 1992, p. 81.
16. X. TANG, C. WU and H. CONRAD, *J. Rheol.* **39** (1995) 1059.
17. H. J. CHOI, M. S. CHO, J. W. KIM, R. M. WEBBER and M. S. JHON, *Inter. J. Mod. Phys.* B **15** (2001) 988.
18. A. GOZDALIK, H. WYCISLIK and J. PLOCHARSKI, *Synthetic Metals* **109** (2000) 147.
19. J. G. YANG and M. S. DISSERTATION, Northwestern Polytechnical University, Xi'an 2001 (in Chinese).
20. D. J. KLINGENBERG, S. V. FRANK and C. F. ZUKOSKI, *J. Chem. Phys.* **94** (1991) 6160.
21. T. HAO, *Adv. Colloid. Inter. Sci.* **97** (2002) 1.

*Received 8 July 2003*
*and accepted 29 January 2004*